ELSEVIER

CrossMark

Localized abnormalities in the cingulum bundle in patients with schizophrenia: A Diffusion Tensor tractography study

Thomas J. Whitford [a,b,1], Sun Woo Lee [b,c,1], Jungsu S. Oh [b,d], Rodrigo de Luis-Garcia [e,f], Peter Savadjiev [b,e], Jorge L. Alvarado [b], Carl-Fredrik Westin [e], Margaret Niznikiewicz [g], Paul G. Nestor [g,h,i], Robert W. McCarley [g], Marek Kubicki [b], Martha E. Shenton [b,h,*]

[a] School of Psychology, University of New South Wales, Sydney, NSW, Australia
[b] Psychiatry Neuroimaging Laboratory, Departments of Psychiatry and Radiology, Brigham and Women's Hospital, Harvard Medical School, Boston, MA, USA
[c] Department of Psychiatry, School of Medicine, Chungnam National University, Daejeon, South Korea
[d] Department of Nuclear Medicine, Asan Medical Center, University of Ulsan College of Medicine, Seoul, South Korea
[e] Laboratory of Mathematics in Imaging, Department of Radiology, Brigham and Women's Hospital, Harvard Medical School, Boston, MA, USA
[f] Laboratorio de Procesado de Imagen, Universidad de Valladolid, Spain
[g] Clinical Neuroscience Division, Laboratory of Neuroscience, Department of Psychiatry, Boston Veterans Affairs Healthcare System, Brockton Division, Brockton, MA, USA and Harvard Medical School, Boston, MA, USA
[h] Boston Veterans Affairs Healthcare System, Brockton Division, Brockton, MA, USA
[i] Department of Psychology, University of Massachusetts, Boston, MA, USA

ARTICLE INFO

ABSTRACT

The cingulum bundle (CB) connects gray matter structures of the limbic system and as such has been implicated in the etiology of schizophrenia. There is growing evidence to suggest that the CB is actually comprised of a conglomeration of discrete sub-connections. The present study aimed to use Diffusion Tensor tractography to subdivide the CB into its constituent sub-connections, and to investigate the structural integrity of these sub-connections in patients with schizophrenia and matched healthy controls. Diffusion Tensor Imaging scans were acquired from 24 patients diagnosed with chronic schizophrenia and 26 matched healthy controls. Deterministic tractography was used in conjunction with FreeSurfer-based regions-of-interest to subdivide the CB into 5 sub-connections (I1 to I5). The patients with schizophrenia exhibited subnormal levels of FA in two cingulum sub-connections, specifically the fibers connecting the rostral and caudal anterior cingulate gyrus (I1) and the fibers connecting the isthmus of the cingulate with the parahippocampal cortex (I4). Furthermore, while FA in the I1 sub-connection was correlated with the severity of patients' positive symptoms (specifically hallucinations and delusions), FA in the I4 sub-connection was correlated with the severity of patients' negative symptoms (specifically affective flattening and anhedonia/asociality). These results support the notion that the CB is a conglomeration of structurally interconnected yet functionally distinct sub-connections, of which only a subset are abnormal in patients with schizophrenia. Furthermore, while acknowledging the fact that the present study only investigated the CB, these results suggest that the positive and negative symptoms of schizophrenia may have distinct neurobiological underpinnings.

1. Introduction

It is notable that many of the cognitive processes known to be abnormal in patients with schizophrenia have been associated with the functioning of the limbic system, such as emotion regulation, emotion processing, self-monitoring, memory and attention. This observation has led to a number of theories that have emphasized the role of limbic system dysfunction in the etiology of schizophrenia, potentially via its role in the integration of cognition and emotion (Anticevic and Corlett, 2012; Coltheart, 2010), and/or sensory and cognitive gating (Bogerts et al., 1985; Grace, 2000).

The limbic system is a phylogenetically ancient neural system comprised of a number of structurally and functionally interconnected gray matter structures (Mega et al., 1997). While the boundaries of the limbic system are somewhat unclear, the limbic system is generally taken to include the anterior cingulate gyrus, involved in emotional processing and error-monitoring (Holroyd et al., 2004; Whalen et al., 2006), the posterior cingulate gyrus, involved in the evaluation of risk and

reward (McCoy and Platt, 2005; Vogt et al., 1992), the isthmus of the cingulate gyrus, involved in memory and pain processing (Nielsen et al., 2005), the parahippocampal cortex, involved in memory (Squire and Zola-Morgan, 1991), and the entorhinal cortex, involved in memory and spatial processing (Eustache et al., 2001; Frank et al., 2000).

The gray matter subcomponents of the limbic cortex are structurally connected with each other via a major white-matter fasciculus called the cingulum bundle (CB). Consistent with the suggestion that schizophrenia is underpinned by a disconnection between the neural processes of emotion, self-monitoring, memory and attention (Andreasen, 1999), abnormalities in the CB and limbic gray matter have consistently been observed in patients with schizophrenia, both directly via microscopy (Benes, 1993) and indirectly with structural MRI (Honea et al., 2005; Koo et al., 2008; Shenton et al., 1992) and Diffusion Tensor Imaging (DTI) (Fujiwara and Murai, 2007; Kubicki et al., 2003; Wang et al., 2004).

Several histological studies of the rat (Jones et al., 2005), cat (Room and Groenewegen, 1986), and primate brain (Baleydier and Mauguiere, 1980, 1985; Mufson and Pandya, 1984; Vogt and Pandya, 1987) suggest that the CB is not structurally homogenous but instead consists of a number of topographically and cytoarchitecturally distinct connections that connect adjacent structures of the limbic system. Given the diverse functions of the limbic system structures, it might be expected that the level of structural abnormality exhibited by schizophrenia patients could vary across the different CB sub-regions. Furthermore, a differential relationship might also be expected between patients' clinical profiles and their degree of structural abnormality in the various CB subregions. To our knowledge, however, neither of these possibilities has been systematically investigated in the schizophrenia literature, possibly because of the technical difficulties associated with delineating the sub-connection of the CB, in vivo, with neuroimaging.

The present study used DTI in conjunction with a tractographybased protocol to delineate and to extract the subcomponents of the CB on the basis of their connectivity with a standardized set of limbic regions-of-interest (ROIs). The integrity of these CB subcomponents was quantified in a group of chronic schizophrenia patients and a matched group of healthy control participants on the basis of the wellestablished DTI metric of Fractional Anisotropy (FA). The relationship between FA and patients' clinical symptoms was also investigated.

2. Materials and methods

2.1. Participants

Twenty-four male patients with chronic schizophrenia were recruited from the Veteran's Affairs (VA) Boston Healthcare System, Brockton Division. The protocols for diagnosis and clinical evaluation have been described in detail elsewhere (Hirayasu et al., 1998; Salisbury et al., 2007). Patient diagnoses were based on the DSM-IV-TR criteria using the Structured Clinical Interview for DSM-IV (SCID) (First et al., 1997), in conjunction with information from medical records. At the time of scanning, all schizophrenia patients were being administered second-generation antipsychotics. Patients' medication history was assessed on the basis of a self-report and a review of the medical record. Patients' clinical symptoms were assessed with the Scale for the Assessment of Positive Symptoms (SAPS; (Andreasen, 1984a)) and the Scale for the Assessment of Negative Symptoms (SANS; (Andreasen, 1984b)). The severity of patients' clinical symptoms was quantified on the basis of their scores on the 4 subscales of the SAPS (hallucinations, delusions, bizarre behavior, positive formal thought disorder) and the 5 subscales of the SANS (affective flattening, alogia, avolition–apathy, anhedonia–asociality, attention). All scales were administered within 2–3 weeks of MRI scanning.

Twenty-six healthy male control subjects were recruited through local newspaper advertisements. The control subjects did not exhibit any Axis I or Axis II psychiatric disorders (as assessed with the Structured Clinical Interview for DSM-IV-TR for Non-patients (SCID-I/NP;

(First et al., 2002)), nor did they report having any first-degree relations with Axis I disorders.

All participants were screened for the following exclusion criteria: left-handedness (Oldfield, 1971), a history of seizures, head trauma with loss of consciousness, neurological disorder including epilepsy, drug or alcohol dependence within the past 5 years, and drug or alcohol abuse within the past year. The patients and healthy controls were matched for age, handedness, parental socio-economic status (Hollingshead, 1965) and estimated pre-morbid IQ, which was calculated on the basis of the Wide-Range Achievement Task (WRAT-3; (Wilkinson, 1993)) — see Table 1. This study was approved by the local Institutional Review Board: VA Boston Healthcare System, Harvard Medical School and Partners Healthcare System. Prior to participation in this study, all participants submitted written informed consent.

2.2. Data acquisition and processing

2.2.1. MRI acquisition and processing

Structural MRIs were acquired on a 3-Tesla whole body MRI Echo speed system General Electric scanner (GE Medical Systems, Milwaukee) at the Brigham and Women's Hospital, Boston, MA. An eight channel coil was used in order to perform parallel imaging using ASSET (Array Spatial Sensitivity Encoding techniques, GE) with a SENSE-factor (speed-up) of 2. The structural MRI acquisition protocol was based on the following pulse sequence: contiguous spoiled gradient-recalled acquisition, T1-weighted, fastSPGR, TR = 7.4 ms, TE = 3 ms, TI = 600, 10 degree flip angle, 25.6 cm^2 field of view, and matrix = 256 × 256. The voxel dimensions were 1 × 1 × 1 mm. Images were manually realigned to the AC/PC line on the mid-sagittal slice.

2.2.2. DTI acquisition and processing

Diffusion-Weighted Images were acquired on the same scanner with the following parameters: TR = 17,000 ms, TE = 78 ms, FOV = 24 cm, 144 × 144 encoding steps, 1.7 mm slice thickness and 85 axial slices. Eight volumes were acquired at b-value 0 s/mm^2 and 51 volumes with diffusion weighting at b-value 900 s/mm^2 along non-collinear and non-coplanar directions. Each of the resulting 59 volumes was then filtered using a Rician Noise filter (Aja-Fernandez et al., 2008). Motion and eddy current correction was performed by co-registering each volume to the first b0 volume using an affine registration algorithm in FSL (http://www.fmrib.ox.ac.uk/fsl). Diffusion Tensor Images (DTIs) were estimated from the Diffusion-Weighted Images in Slicer v2.8 (http://www.slicer.org), on the basis of a weighted-least-squares estimation.

2.2.3. Definition of the six limbic regions-of-interest using FreeSurfer

FreeSurfer (v4.2.0; http://surfer.nmr.mgh.harvard.edu/) was used to parcellate each participant's T1-weighted MRI into 34 neocortical regions (Fischl et al., 2004). Following an automated and manually-validated skull-stripping procedure, the cortical surface of each participant's MRI was inflated into a sphere for the purpose of

Table 1
Demographic information for the 24 schizophrenia patients and 26 healthy control participants. Cells show the mean and standard deviation.

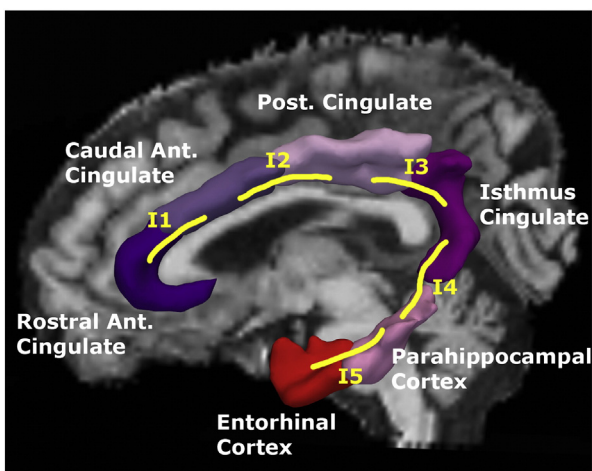|	SZ (n = 24)	HC (n = 26)	SZ vs HC	
			t-Value	p
Age (years)	39.69 (9.80)	37.38 (10.97)	0.789	0.434
Gender	100% male	100% male	–	–
Education (years)	13.21 (1.81)	15.34 (5.11)	2.028	0.048
Parental SES	2.60 (1.56)	2.30 (1.11)	0.905	0.370
Pre-morbid IQ	98.43 (12.33)	104.44 (13.01)	1.221	0.232
Age-of-onset (years)	23.18 (5.01)	–	–	–
Duration-of-illness (years)	17.39 (10.39)	–	–	–
Medication dosage (CPZ)	189 (280)	–	–	–

registering it to an atlas. These inflated representations were then segmented into 34 neocortical regions. Each participant's FreeSurfer segmentation was co-registered to their DTI scan using both an affine registration and a non-linear deformation.

The sub-regions of the CB were identified on the basis of the gray matter regions they connected (see Fig. 1). The following six limbic gray-matter ROIs were extracted from each participant's co-registered FreeSurfer label map: (1) Rostral Anterior Cingulate Gyrus (rACG), (2) Caudal Anterior Cingulate Gyrus (cACG), (3) Posterior Cingulate Gyrus (PCG), (4) Isthmus of Cingulate Gyrus (ICG), (5) Parahippocampal Cortex (PPH), (6) Entorhinal Cortex (ENT). In order to account for registration inaccuracies between each participant's DTI and the six FreeSurfer label-maps, an automatic correction algorithm was developed based on previously described segmentation approaches (de Luis-Garcia and Alberola-Lopez, 2007; Paragios and Deriche, 2002). In a Bayesian setting, the tensor features (shape and orientation) were assumed to follow a Gaussian distribution, and a level set evolution was designed to maximize an energy functional related to the a posteriori frame partition; that is, we obtained the most likely segmentation given the image data and Gaussian model. For this application, the tensor orientation information was weighed with a higher factor, which enabled the boundaries of the CB to be accurately determined.

2.2.4. Tractography and extraction of the CB sub-connections

Each participant's DTI underwent the following processing protocols in Slicer (v.2.8; http://www.slicer.org/):

1. *Whole-brain tractography:* Deterministic (streamline) tractography was performed from every putatively white matter voxel within each participant's Fractional Anisotropy (FA) image (Whitford et al., 2011). Specifically, tractography was initiated from every voxel with an FA value of >0.1 and proceeded in 0.17 mm steps (step size) following the direction defined by the principal eigenvector at that voxel. Tractography was terminated as soon as the FA fell below 0.1 (the stopping criterion) and fibers shorter than 10 mm in length were discarded from the analysis. The basic procedure used for deterministic tractography has been described elsewhere (Whitford et al., 2011).

2. *Extraction of CB subcomponents:* The six FreeSurfer ROIs were used to extract five subcomponents of the CB from each participant's whole-brain tractography image. The five sub-connections (i.e., I1 through I5, described below) were defined as follows:
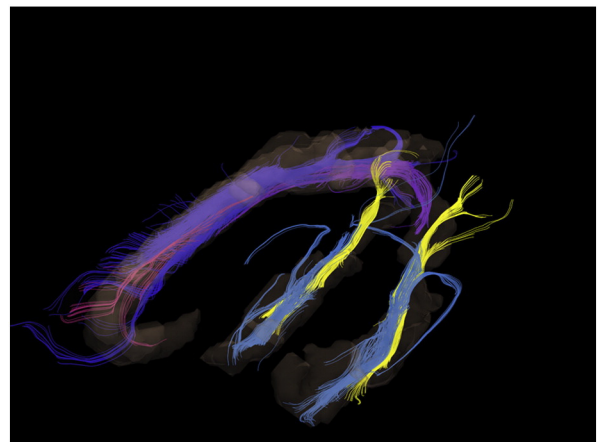
   – I1 was defined as the fibers connecting the Rostral Anterior Cingulate Gyrus (rACG) with the Caudal Anterior Cingulate Gyrus (cACG) ROIs.
   – I2 was defined as the fibers connecting the Caudal Anterior Cingulate Gyrus (cACG) and Posterior Cingulate Gyrus (PCG) ROIs.
   – I3 was defined as the fibers connecting the Posterior Cingulate Gyrus (PCG) and the Isthmus of Cingulate Gyrus (ICG) ROIs.
   – I4 was defined as the fibers connecting the Isthmus of Cingulate Gyrus (ICG) and the Parahippocampal Cortex (PPH) ROIs.
   – I5 was defined as the fibers connecting the Parahippocampal Cortex (PPH) and the Entorhinal Cortex (ENT) ROIs.

Fig. 2, which was generated in Slicer 2.8, shows an in-vivo 3D-fiber reconstruction for the 5 CB sub-connections.

1. *Calculation of Fractional Anisotropy:* Mean Fractional Anisotropy (FA) was calculated for each of the five sub-connections. FA, which is a widely used metric of white-matter integrity, was calculated at every voxel in each participant's DTI as per the protocol of Basser and colleagues (Basser et al., 1994). For each of the five sub-connections, mean FA was calculated for each participant by averaging the FA values of all voxels through which any of the fibers of a given sub-connection passed.

2.3. Data analysis

SPSS for Windows (v.17; www.spss.com) was used for the statistical analysis. An initial mixed-model Analysis-of-Variance (ANOVA) was used to investigate for groupwise differences in FA in the entire CB, with Group (schizophrenia vs. control) as the between-subjects factor and Hemisphere (left vs. right) as the within-subjects factor. A primary analysis used a mixed-model ANOVA to investigate for groupwise differences in FA across the 5 sub-components of the CB. In this analysis, Sub-connection (I1 through I5) and Hemisphere (left vs. right) were entered as within-subjects factors, and Group (schizophrenia vs. control) was entered a between-subjects factor. Greenhouse–Geisser corrections were applied to all analyses where the assumption of sphericity was violated. Any significant main effects or interactions were explored further using post hoc independent samples t-tests. Pearson's correlations were used to evaluate the relationship between the severity of patients' clinical symptoms – as assessed by the 4 subscales of the SAPS and 5 subscales of the SANS – and FA in any sub-connection identified (by the post hoc t-tests) as being structurally abnormal in the patient group.

Fig. 1. Extracting the sub-connections of the cingulum bundle (CB) using streamline tractography with inclusion/exclusion ROIs. The six modified FreeSurfer ROIs are shown overlaid onto a T1-weighted structural MRI. The rostral anterior cingulate (rACG) is shown in deep purple, the caudal anterior cingulate (cACG) is shown in purple, the posterior cingulate (PCG) is shown in light purple, the isthmus of the cingulate (ICG) is shown in dark pink, the parahippocampal cortex (PPH) is shown in light pink and the entorhinal cortex (ENT) is shown in light pink. Schematics of the five CB sub-connections (I1 through I5) are shown as short yellow bars.

Fig. 2. In vivo 3D-fiber reconstruction for 5 CB sub-connections by using Slicer 2.8. 3D image is shown from superior-lateral view. Color coding is as follows. I1: light pink, I2: blue, I3: light purple, I4: yellow, I5: light blue.

3. Results

The initial analysis of the entire CB revealed a significant main effect of Group (F(1, 48) = 5.109, p = .028), which indicated that the patients with schizophrenia exhibited FA reductions in the whole CB, relative to the healthy control participants. There was also a main effect of Hemisphere (F(1,48) = 29.092, p < .001), which indicated that FA in the left CB was higher than FA in the right CB, when collapsing across Group. No significant Group × Hemisphere interaction was observed (F(1,48) = 1.280, p = .263), which indicated that the main effect of Hemisphere (i.e., left CB having higher FA than right CB) was comparable across the schizophrenia and healthy control groups.

With regard to the primary (sub-regional) analysis, deterministic tractography failed to identify fibers for one or more of the 5 CB sub-connections for 4 schizophrenia patients and 7 healthy controls, and these participants were removed from the subsequent analysis. The sub-regional analysis revealed a significant main effect of Group (F(1,37) = 4.944, p = 0.032). Post hoc t-tests revealed that this main effect of Group was driven by the patients with schizophrenia having significantly lower levels of FA in right I1 (t(47) = 2.52, p = 0.015), and right I4 (t(40) = 2.46, p = 0.018) relative to the healthy controls — see Fig. 3. The ANOVA also revealed a significant main effect of Sub-connection (F(4,148) = 43.247, p < 0.001), which indicated that the five sub-connections differed in terms of their mean FA. As can been seen in Fig. 3, this main effect was caused by sub-connection I2 having a markedly higher mean FA than any of the other four sub-components. The Group × Sub-connection interaction was not significant (F(4,148) = 1.142, p = .322), which indicated that the main effect of Sub-connection (i.e., I2 having higher FA than the other sub-connections) did not differ between the schizophrenia and healthy control groups. There was a significant main effect of Hemisphere (F(1,37) = 238.494, p < .001), which reflected the sub-connections of the left CB having higher FA than the sub-connections of the right CB, collapsing across Group — see Fig. 3. The Group × Hemisphere interaction was not significant (F(1,37) = .361, p = .551), which indicated that the main effect of Hemisphere did not differ between the schizophrenia and healthy control groups. Finally, the Group × Hemisphere × Sub-connection interaction was also not significant (F(4,148) = 1.008, p = .375).

The FA of the two sub-connections in which the patients exhibited FA reductions relative to the healthy controls – namely right I1 and right I4 – was correlated with patients' scores on the 4 subscales of the SAPS (hallucinations, delusions, bizarre behavior, and positive formal thought disorder) and the 5 subscales of the SANS (affective flattening, alogia, avolition–apathy, anhedonia–asociality, and attention). Notably, there was a marked dissociation between the two sub-connections of interest in the nature of the observed correlations with clinical symptoms. More specifically, the right I1 sub-connection was observed to be significantly negatively correlated with the hallucinations subscale of the SAPS (r(24) = −.485, p = .014), with a trend towards a negative correlation with the delusions subscale of the SAPS (r(24) = −.356, p = .081). The correlation with hallucinations remained statistically significant when controlling for patients' CPZ-equivalent medication dosage (partial r(15) = −.483, p = .049), while the correlation with delusions changed from a trend to being statistically significant when controlling for CPZ-medication dosage (partial r(15) = −.503, p = 0.04). In contrast to the correlations with positive symptoms observed in I1, the right I4 sub-connection was significantly negatively correlated with two subscales of the SANS, namely affective flattening (r(20) = −.461, p = 0.041), and anhedonia/asociality (r(20) = −.588, p = .006). Both of these correlations remained statistically significant when controlling for patients' CPZ-equivalent medication dosage
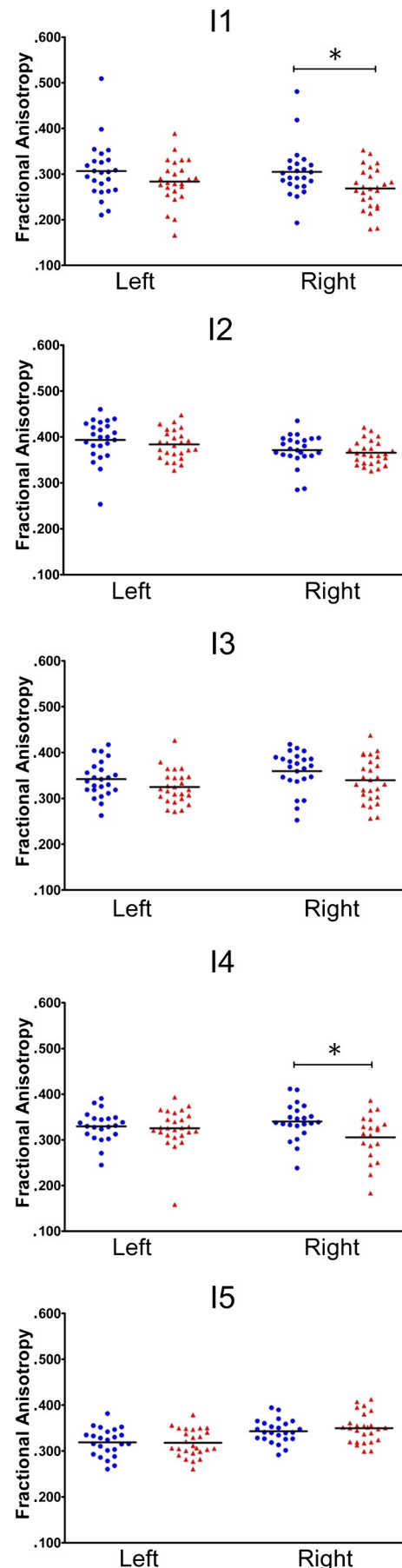
Fig. 3. Between-group differences in FA in the five CB sub-connections (I1 through I5). Schizophrenia patients are shown as red triangles and control participants are shown as blue circles. The black bars represent the group means. *p < 0.05.

(affective flattening: partial r(16) = −.512, p = .03; anhedonia/asociality r(16) = −.539, p = .021). Scatterplots illustrating the significant correlations between patients FA in the two affected CB-subregions (i.e., right I1 and right I4) and the severity of their clinical symptoms, both positive and negative (as assessed with the subscales of the SAPS and SANS) are presented in Fig. 4.

4. Discussion

The primary aim of the present study was to use Diffusion Tensor tractography to subdivide the cingulum bundle into its constituent sub-connections, and to compare the structural integrity of these sub-connections between patients with schizophrenia and matched healthy controls. Of the 5 identified CB sub-connections, only two were identified as being structurally abnormal in patients diagnosed with schizophrenia: specifically, the fibers connecting the rostral and caudal portions of the anterior cingulate gyrus (right I1), and the fibers connecting the isthmus of the cingulate gyrus with the parahippocampal cortex (right I4). There was a marked difference in the nature of the clinical correlations for each of these two affected sub-connections. Specifically, while the right I1 sub-connection was correlated with the severity of patients' *positive* symptoms, the right I4 sub-connection was correlated with the severity of patients' *negative* symptoms.

While numerous previous studies have observed FA abnormalities in schizophrenia patients in the CB as a whole (Fujiwara and Murai, 2007; Kubicki et al., 2003; Wang et al., 2004), there is growing evidence to suggest that not all CB sub-regions are equally affected in the disorder. For example, Fujiwara and Murai (2007) used tractography in conjunction with manually-defined ROIs to distinguish between the anterior

and posterior cingulum bundles, and found that while patients with chronic schizophrenia exhibited significant FA reductions in both the anterior and posterior cingula (relative to controls), these FA reductions were more severe in the anterior cingulum and particularly the right hemisphere — consistent with the results of the present study. Similarly, Takei et al. (2009) used a similar approach to segment the CB into the pregenual and dorsal CB and found that while schizophrenia patients showed reduced integrity in both segments, the integrity of patients' dorsal CB, but not their pregenual CB, was associated with their performance on a Stroop task, suggesting a functional specialization within the CB. More recently, Abdul-Rahman, Qui and Sim (Abdul-Rahman et al., 2011) used a more automated tractography-based approach to segment the CB into 4 sub-regions and found that patients with chronic schizophrenia exhibited FA reductions in the right 'anterior cingulum': a region that encompasses our I1 CB sub-division. Thus there is growing evidence that the CB consists of several functionally discrete sub-fascicles, and that not all CB sub-components are equally affected in schizophrenia.

The results of the present study indicated that the schizophrenia patients exhibited structural abnormalities in two discrete sub-fascicles in the CB. The first of the affected sub-fascicles, named by us as I1, consisted of fibers connecting the rostral and caudal regions of the anterior cingulate cortex (ACC). While the rostral ACC is believed to be involved in assessing the salience of emotional information and the regulation of emotional responses (Bissiere et al., 2008; Devinsky et al., 1995) – a role reflected in its connections with the amygdala, periaqueductal gray, nucleus accumbens, and hypothalamus – the caudal ACC is believed to play more of a cognitive role, as reflected in its functional activity during memory and executive functioning tasks
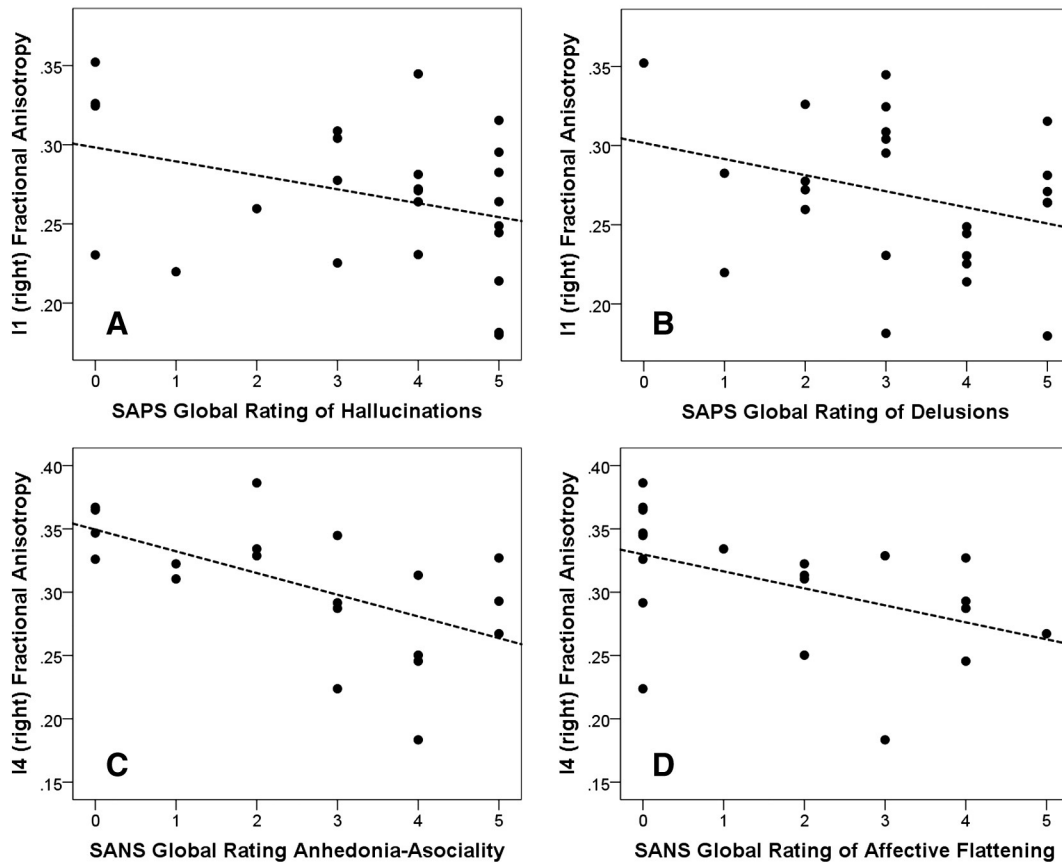
Fig. 4. Scatterplots illustrating the significant correlations observed between FA and clinical symptoms in the 24 schizophrenia patients. Panel A shows the significant negative correlation between FA in the 'right I1' CB subregion and patients' score on the Hallucinations subscale of the SAPS. Panel B shows the significant negative correlation between FA in the 'right I1' CB subregion and patients' score on the Delusions subscale of the SAPS. Panel C shows the significant negative correlation between FA in the 'right I4' CB subregion and patients' score on the Anhedonia–Asociality subscale of the SANS. Panel D shows the significant negative correlation between FA in the 'right I4' CB subregion and patients' score on the Affective Flattening subscale of the SANS.

and its connections with the prefrontal cortex (Bush et al., 2000). In addition to these FA reductions, patients' FA in sub-fascicle I1 was found to be significantly negatively correlated with the severity of their positive symptoms — specifically, hallucinations and delusions. In light of the aforementioned roles of the rostral and caudal ACC, this finding is consistent with the idea that the psychotic symptoms of schizophrenia ultimately arise from an abnormal interaction between cognition and emotion, such as has been suggested previously (Anticevic and Corlett, 2012; Coltheart, 2010).

The second affected CB sub-connection, named by us as I4, consisted of fibers connecting the isthmus of the cingulate gyrus with the parahippocampal cortex. Both of these brain regions are believed to be involved in memory formation and retrieval. The parahippocampal cortex is known to play an important role in the encoding and retrieval of long-term memories, particularly declarative memories (Squire and Zola-Morgan, 1991). While the functions of the isthmus are less well understood, it is also believed to play a role in memory, particularly spatial memory. For example, there is evidence to suggest that damage to the isthmus can result in topographical disorientation, which is an inability to navigate familiar surroundings (Katayama et al., 1999). In light of the memory-related functions of these regions, it is interesting to note that – in stark contrast to the clinical correlations observed with I1 – patients' FA in I4 was significantly negatively correlated with the severity of their *negative* symptoms – specifically affective flattening and anhedonia/asociality – but was uncorrelated with the severity of their positive symptoms. In light of the aforementioned role of the isthmus/parahippocampal cortex in memory formation and retrieval, the observed correlation is consistent with previous studies which have identified a relationship between negative symptom severity and memory impairment — particularly spatial working memory (Carter et al., 1996; McCreadie et al., 1997; Pantelis et al., 2001). Taken together, these results at least tentatively suggest that the positive and negative symptoms of schizophrenia may be underpinned by brain abnormalities that are – to some extent – structurally and functionally distinct. However, it must be emphasized that the present study only investigated a single fiber bundle – the cingulum – and thus any attempt to generalize the results of the observed correlations should be treated with the upmost caution until the results are replicated.

The notion that the CB is actually a conglomeration of structurally and functionally distinct sub-fascicles – as opposed to a homogenous fiber bundle – is supported by numerous in vitro studies from the animal literature, many of which have employed anterograde and retrograde tracing techniques to directly visualize the axonal connections between the gray matter structures of the limbic system (Baleydier and Mauguiere, 1980, 1985; Morecraft et al., 2004, 2012; Pandya and Seltzer, 1982; Vogt and Pandya, 1987; Vogt et al., 1979). While the actual number of CB sub-fascicles has not been definitively established, previous research from the animal literature suggests that the true number is likely to be higher than the five sub-connections extracted in the present study. For example, Jones et al. (2005) used anterograde tracing to explore the patterns of fiber connection within the rat cingulate cortex and found it could be sub-divided into at least 13 discrete sub-regions on the basis of the cytoarchitectonic characteristics of the tissue and the distinctive patterns of axonal projection. While the relatively course spatial resolution currently afforded by DTI, combined with the difficulties inherent in registering pre-defined regions-of-interest to variably shaped MR images clearly poses a major challenge for the correct and complete segmentation of the CB on the basis of DTI, recent advances in neuroimaging – such as evinced by the recent publication of MR sequences capable of imaging the laminar structure of the cortex (Duyn et al., 2007) – suggest that achieving this aim may become a realistic possibility in the not too distant future.

There were at least four limitations of the present study. The first limitation is that all of the patients diagnosed with schizophrenia were taking antipsychotic medication at the time of scanning, and generally had been ill for several years. While both observed correlations remained statistically significant when controlling for patients' CPZ-equivalent medication dosages, the possibility that antipsychotic exposure underpinned patients' structural brain abnormalities cannot be discounted. Secondly, all of the participants in this study were male. While this is in some ways advantageous – for example, in terms of minimizing the between-subject variability in brain structure – it clearly limits the generalizability of the results. Thirdly, the present study only investigated the structural connections between the cortical components of the limbic system. Connections between the sub-cortical components of the limbic system (such as the mammillary bodies and amygdala) were not investigated, primarily because of the difficulties associated with reliably tracking sub-thalamic fibers. We hope to address this limitation in future studies with the aid of novel tractographic methods such as multi-tensor tractography (Malcolm et al., 2009). Fourthly, it must be acknowledged that our sub-division of the CB into 5 sub-components was at least somewhat arbitrary. While our CB were designed to loosely map onto the schema of Jones et al. (2005) (who distinguished between 6 'global' subcomponents) they were primarily selected because of the fact that they were reliably definable on the basis of an established and replicable procedure (i.e., FreeSurfer ROIs). While it may have been possible to more closely match Jones et al.'s (2005) schema by using manually-defined ROIs, the fact that this schema was used to describe the rat brain and the absence of any reliable and established anatomical landmarks for these CB subdivisions in humans made this approach unfeasible for the present study.

In conclusion, this study used deterministic fiber tractography in conjunction with Diffusion Tensor Imaging to subdivide the cingulum bundle into structurally discrete sub-connections and to compare the FA of these sub-connections between patients with chronic schizophrenia and matched healthy controls. The schizophrenia patients exhibited subnormal levels of FA in two CB sub-connections — specifically the fibers connecting the rostral and caudal anterior cingulate gyri (I1) and the fibers connecting the isthmus of the cingulate with the parahippocampal cortex (I4). Notably, FA in I1 was correlated with the severity of patients' positive symptoms but not their negative symptoms, while the converse pattern of correlation was observed in I4, suggesting that the positive and negative symptoms of schizophrenia may be underpinned by white matter abnormalities that are, to some extent, structurally distinct. In conclusion, these results support the suggestion that the CB is a conglomeration of structurally interconnected yet functionally distinct sub-connections of which only a discrete subset are abnormal in patients with schizophrenia.

References

Abdul-Rahman, M.F., Qiu, A., Sim, K., 2011. Regionally specific white matter disruptions of fornix and cingulum in schizophrenia. PLoS One 6, e18652.

Aja-Fernandez, S., Niethammer, M., Kubicki, M., Shenton, M.E., Westin, C.F., 2008. Restoration of DWI data using a Rician LMMSE estimator. IEEE Trans. Med. Imaging 27, 1389–1403.

Andreasen, N.C., 1984a. Scale for the Assessment of Positive Symptoms (SAPS). University of Iowa, Iowa City.

Andreasen, N.C., 1984b. Scale for the Assessment of Negative Symptoms (SANS). University of Iowa, Iowa City.

Andreasen, N., 1999. A unitary model of schizophrenia: Bleuler's "fragmented phrene" as schizencephaly. Arch. Gen. Psychiatry 56, 781–787.

Anticevic, A., Corlett, P.R., 2012. Cognition–emotion dysinteraction in schizophrenia. Front. Psychol. 3, 392.

Baleydier, C., Mauguiere, F., 1980. The duality of the cingulate gyrus in monkey. Neuroanatomical study and functional hypothesis. Brain 103, 525–554.

Baleydier, C., Mauguiere, F., 1985. Anatomical evidence for medial pulvinar connections with the posterior cingulate cortex, the retrosplenial area, and the posterior parahippocampal gyrus in monkeys. J. Comp. Neurol. 232, 219–228.

Basser, P.J., Mattiello, J., LeBihan, D., 1994. MR diffusion tensor spectroscopy and imaging. Biophys. J. 66, 259–267.

Benes, F.M., 1993. Neurobiological investigations in cingulate cortex of schizophrenic brain. Schizophr. Bull. 19, 537–549.

Bissiere, S., Plachta, N., Hoyer, D., McAllister, K.H., Olpe, H.R., et al., 2008. The rostral anterior cingulate cortex modulates the efficiency of amygdala-dependent fear learning. Biol. Psychiatry 63, 821–831.

Bogerts, B., Meertz, E., Schonfeldt-Bausch, R., 1985. Basal ganglia and limbic system pathology in schizophrenia. A morphometric study of brain volume and shrinkage. Arch. Gen. Psychiatry 42, 784–791.

Bush, G., Luu, P., Posner, M.I., 2000. Cognitive and emotional influences in anterior cingulate cortex. Trends Cogn. Sci. 4, 215–222.

Carter, C., Robertson, L., Nordahl, T., Chaderjian, M., Kraft, L., et al., 1996. Spatial working memory deficits and their relationship to negative symptoms in unmedicated schizophrenia patients. Biol. Psychiatry 40, 930–932.

Coltheart, M., 2010. The neuropsychology of delusions. Ann. N. Y. Acad. Sci. 1191, 16–26.

de Luis-Garcia, R., Alberola-Lopez, C., 2007. Mixtures of Gaussians on tensor fields for DT-MRI segmentation. Med. Image Comput. Comput. Assist. Interv. 10, 319–326.

Devinsky, O., Morrell, M.J., Vogt, B.A., 1995. Contributions of anterior cingulate cortex to behaviour. Brain 118, 279–306.

Duyn, J.H., van Gelderen, P., Li, T.Q., de Zwart, J.A., Koretsky, A.P., et al., 2007. High-field MRI of brain cortical substructure based on signal phase. Proc. Natl. Acad. Sci. U. S. A. 104, 11796–11801.

Eustache, F., Desgranges, B., Giffard, B., de la Sayette, V., Baron, J.C., 2001. Entorhinal cortex disruption causes memory deficit in early Alzheimer's disease as shown by PET. Neuroreport 12, 683–685.

First, M., Spitzer, R., Gibbon, M., Williams, J., 1997. Structured Clinical Interview for DSM-IV-TR Axis I Disorders (SCID-I), Clinician Version. American Psychiatric Publishing, Inc.

First, M.B., Spitzer, R.L., Gibbon, M., Williams, B.J., 2002. Structured Clinical Interview for DSM-IV-TR Axis I Disorders, Research Version, Non-patient Edition. Biometrics Research, New York State Psychiatric Institute, New York, (SCID-I/NP).

Fischl, B., van der Kouwe, A., Destrieux, C., Halgren, E., Segonne, F., et al., 2004. Automatically parcellating the human cerebral cortex. Cereb. Cortex 14, 11–22.

Frank, L., Brown, E., Wilson, M., 2000. Trajectory encoding in the hippocampus and entorhinal cortex. Neuron 27, 169–178.

Fujiwara, H., Murai, T., 2007. Anterior and posterior cingulum abnormalities and their association with psychopathology in schizophrenia: a diffusion tensor imaging study. Schizophr. Res. 95, 215–222.

Grace, A., 2000. Gating of information flow within the limbic system and the pathophysiology of schizophrenia. Brain Res. Brain Res. Rev. 31, 330–341.

Hirayasu, Y., Shenton, M.E., Salisbury, D.F., Dickey, C.C., Fischer, I.A., et al., 1998. Lower left temporal lobe MRI volumes in patients with first-episode schizophrenia compared with psychotic patients with first-episode affective disorder and normal subjects. Am. J. Psychiatr. 155, 1384–1391.

Hollingshead, A., 1965. Two Factor Index of Social Position. Yale Station, New Haven.

Holroyd, C.B., Nieuwenhuis, S., Yeung, N., Nystrom, L., Mars, R.B., et al., 2004. Dorsal anterior cingulate cortex shows fMRI response to internal and external error signals. Nat. Neurosci. 7, 497–498.

Honea, R., Crow, T.J., Passingham, D., Mackay, C.E., 2005. Regional deficits in brain volume in schizophrenia: a meta-analysis of voxel-based morphometry studies. Am. J. Psychiatr. 162, 2233–2245.

Jones, B.F., Groenewegen, H.J., Witter, M.P., 2005. Intrinsic connections of the cingulate cortex in the rat suggest the existence of multiple functionally segregated networks. Neuroscience 133, 193–207.

Katayama, K., Takahashi, N., Ogawara, K., Hattori, T., 1999. Pure topographical disorientation due to right posterior cingulate lesion. Cortex 35, 279–282.

Koo, M.S., Levitt, J.J., Salisbury, D.F., Nakamura, M., Shenton, M.E., et al., 2008. A cross-sectional and longitudinal magnetic resonance imaging study of cingulate gyrus gray matter volume abnormalities in first-episode schizophrenia and first-episode affective psychosis. Arch. Gen. Psychiatry 65, 746–760.

Kubicki, M., Westin, C., Nestor, P., Wible, C., Frumin, M., et al., 2003. Cingulate fasciculus integrity disruption in schizophrenia: a magnetic resonance diffusion tensor imaging study. Biol. Psychiatry 54, 1171–1180.

Malcolm, J.G., Shenton, M.E., Rathi, Y., 2009. Two-tensor tractography using a constrained filter. Med. Image Comput. Comput. Assist. Interv. 12, 894–902.

McCoy, A., Platt, M., 2005. Risk-sensitive neurons in macaque posterior cingulate cortex. Nat. Neurosci. 8, 1220–1227.

McCreadie, R.G., Latha, S., Thara, R., Padmavathi, R., Ayankaran, J.R., 1997. Poor memory, negative symptoms and abnormal movements in never-treated Indian patients with schizophrenia. Br. J. Psychiatry 171, 360–363.

Mega, M.S., Cummings, J.L., Salloway, S., Malloy, P., 1997. The limbic system: an anatomic, phylogenetic, and clinical perspective. J. Neuropsychiatry Clin. Neurosci. 9, 315–330.

Morecraft, R.J., Cipolloni, P.B., Stilwell-Morecraft, K.S., Gedney, M.T., Pandya, D.N., 2004. Cytoarchitecture and cortical connections of the posterior cingulate and adjacent somatosensory fields in the rhesus monkey. J. Comp. Neurol. 469, 37–69.

Morecraft, R.J., Stilwell-Morecraft, K.S., Cipolloni, P.B., Ge, J., McNeal, D.W., et al., 2012. Cytoarchitecture and cortical connections of the anterior cingulate and adjacent somatomotor fields in the rhesus monkey. Brain Res. Bull. 87, 457–497.

Mufson, E.J., Pandya, D.N., 1984. Some observations on the course and composition of the cingulum bundle in the rhesus monkey. J. Comp. Neurol. 225, 31–43.

Nielsen, F.A., Balslev, D., Hansen, L.K., 2005. Mining the posterior cingulate: segregation between memory and pain components. NeuroImage 27, 520–532.

Oldfield, R.C., 1971. The assessment and analysis of handedness: the Edinburgh inventory. Neuropsychologia 9, 97–113.

Pandya, D.N., Seltzer, B., 1982. Intrinsic connections and architectonics of posterior parietal cortex in the rhesus monkey. J. Comp. Neurol. 204, 196–210.

Pantelis, C., Stuart, G.W., Nelson, H.E., Robbins, T.W., Barnes, T.R., 2001. Spatial working memory deficits in schizophrenia: relationship with tardive dyskinesia and negative symptoms. Am. J. Psychiatry 158, 1276–1285.

Paragios, N., Deriche, R., 2002. Geodesic active regions: a new framework to deal with frame partition problems in computer vision. J. Vis. Commun. Image Represent. 13, 249–268.

Room, P., Groenewegen, H.J., 1986. Connections of the parahippocampal cortex. I. Cortical afferents. J. Comp. Neurol. 251, 415–450.

Salisbury, D., Kuroki, N., Kasai, K., Shenton, M., McCarley, R., 2007. Progressive and inter-related functional and structural evidence of post-onset brain reduction in schizophrenia. Arch. Gen. Psychiatry 64, 521–529.

Shenton, M.E., Kikinis, R., Jolesz, F.A., Pollak, S.D., LeMay, M., et al., 1992. Abnormalities of the left temporal lobe and thought disorder in schizophrenia: a quantitative magnetic resonance imaging study. N. Engl. J. Med. 327, 604–612.

Squire, L.R., Zola-Morgan, S., 1991. The medial temporal lobe memory system. Science 253, 1380–1386.

Takei, K., Yamasue, H., Abe, O., Yamada, H., Inoue, H., Suga, M., Moroi, M., Sasaki, H., Aoki, S., Kasai, K., 2009. Structural disruption of the dorsal cingulum bundle is associated with impaired Stroop performance in patients with schizophrenia. Schizophr. Res. 114, 119–127.

Vogt, B.A., Pandya, D.N., 1987. Cingulate cortex of the rhesus monkey: II. Cortical afferents. J. Comp. Neurol. 262, 271–289.

Vogt, B.A., Rosene, D.L., Pandya, D.N., 1979. Thalamic and cortical afferents differentiate anterior from posterior cingulate cortex in the monkey. Science 204, 205–207.

Vogt, B.A., Finch, D.M., Olson, C.R., 1992. Functional heterogeneity in cingulate cortex: the anterior executive and posterior evaluative regions. Cereb. Cortex 2, 435–443.

Wang, F., Sun, Z., Cui, L., Du, X., Wang, X., et al., 2004. Anterior cingulum abnormalities in male patients with schizophrenia determined through diffusion tensor imaging. Am. J. Psychiatry 161, 573–575.

Whalen, P.J., Bush, G., Shin, L.M., Rauch, S.L., 2006. The emotional counting Stroop: a task for assessing emotional interference during brain imaging. Nat. Protoc. 1, 293–296.

Whitford, T.J., Savadjiev, P., Kubicki, M., O'Donnell, L.J., Terry, D.P., et al., 2011. Fiber geometry in the corpus callosum in schizophrenia: evidence for transcallosal misconnection. Schizophr. Res. 132, 69–74.

Wilkinson, G., 1993. The Wide Range Achievement Test — Revision 3. Jastak Association, Wilmington, DE.